中國機械工程學刊第四十二卷第三期第 245~253 頁(民國一百一十年)
Journal of the Chinese Society of Mechanical Engineers, Vol.42, No.3, pp 245~253 (2021)

Hydromagnetic Stability of a General Viscous Fluid Film With Weakly Nonlinear Effects on a Rotating Vertical Cylinder

Ming-Che Lin* and Po-Jen Cheng**

Keywords：hydromagnetic stability, Hartmann number, general viscous fluid

ABSTRACT

This paper examines the hydromagnetic stability of a general viscous fluid film with weakly nonlinear effects on a rotating vertical cylinder. The power-law fluid model under an applied uniform magnetic field is used to provide a mathematical description instead of the rheology of polymer resist films. Long-wave perturbation techniques are used to derive the dimensionless generalized nonlinear kinematic equation to represent the physical coating flow. The Ginzburg-Landau equation is applied to numerically calculate pattern formation and illustrate necessary threshold conditions of the critical flow states. The influences of polymer resist films with hydromagnetic stability are studied in terms of the Hartmann constant, m, Rossby number, Ro and flow index, n on weakly nonlinear stability with a small Reynolds number. Moreover, The enhanced magnetic effects are found to the material flows as a dilatant fluid is more stable than a pseudo plastic fluid with the same coating flow.

INTRODUCTION

Using magnetic fields to stabilize film flows avoids the need for mechanical or electrical contact with the fluid, and allows for easy control of the coating film thickness and other properties. However, achieving hydromagnetic stability in a coating flow is subject to a range of possible influences such as centrifugal forces, magnetohynamic forces, inertia and viscous film stress. In recent years, considerable interest has focused on the use of hydromagnetic effects in rotating coating processes for a range of industrial applications (VeeraKrishna, Sravanthi & ReddyGorla, 2020; Garmroodi, Ahmadpour & Talati, 2019; Jiang, Shen, Xu, Wang & Tian, 2019; Khan, Islam, Shah, Khan, Bonyah, Jan & Khan, 2017; Perez, Laroze, Diaz & Mancini, 2014; Singh, 2000).

Linear stability theory can be used to identify instability in a film flow but cannot be used to predict disturbances just exceeding the threshold, and weak nonlinear theory describes the evolution of the most unstable linear mode. Relatively simple amplitude evolution equations such as the Ginzburg-Landau equation (GLE) can be used to analyze the spatial-temporal dynamics of complex flows. GLE governs the finite amplitude evolution of instability waves in a large variety of dissipative systems close to criticality. Due to its simplicity and completeness, GLE has been used in numerous investigations of film flow in weakly stable or instable conditions for different physical systems (Yıldırım, Biswas, Jawad, Ekici, Alzahrani & Belic, 2020; Kozitskiy, 2020; Xu, Zou & Huang, 2019; Cipolatti, Dickstein & Puel, 2015; Schewe, 2013).

Several mathematical models have been used to fit the characteristics of some non-Newtonian fluids in terms of coating flow (Acrivos, Shah & Petersen, 1960; Burgess & Wilson, 1996; Liu, Chen & Wang, 2009). In general, polymer resist films such as photo resists, dielectrics and protective coatings show that viscosity is strongly correlated to the rate of coating process deformation. Appropriate mathematical models can be derived from general viscous fluids to describe the actual film flow characteristics for the rheology of new materials dependant on the rate of deformation. The most widely used mathematical model for general viscous fluids is the power-law constitutive model (Chhabra & Richardson, 2008), which is typically used to describe behaviors such as the material flows of pseudo plastic fluids $(n<1)$ for shear thinning or as dilatant fluids $(n>1)$ for shear thickening characteristics. The simplicity of this model has led to its increased use in experimental and theoretical analysis (Zou, Håkansson & Cvetkovic, 2020; Mahmood, Bilal, Majeed, Khan & Sherif, 2019; Sadigh, Paygozar, Silva & VakiliTahami, 2019; Agassi, 2015).

While most photo resists such as non-Newtonian

Paper Received May, 2020. Revised June, 2020, Accepted July, 2020, Author for Correspondence: Ming-Che Lin.
* *Associate Professor, Department of Mechanical Engineering(Jiangong Campus), National Kaohsiung University of Science and Technology, Kaohsiung, Taiwan, R.O.C.*

** *Professor, Department of Mechanical Engineering, Far-East University, Tainan, Taiwan 74448, R.O.C.*

materials show shear thinning, some show shear thickening due to concentrated suspensions. The rheological properties of a coating liquid can affect the nature of the flow and consequently alter the performance of the coating system. Thickening often induces flow instability and irreversibility. The present study presents the hydromagnetic stability of polymer resist films with weakly nonlinear effects on a vertical rotating coating process. Several previous works have examined the stability of cylindrical rotating systems (Chen, Chen & Yang, 2004; Chen, Chen & Yang, 2005), and the results of the present study provide new modeling of multiphysics process into general viscous fluid films with weakly nonlinear effects on a rotating vertical cylinder.

The remainder of this paper is organized as follows. Section 2 presents the generalized nonlinear kinematic equation of an electrically conductive polymer resist film flowing on a vertical rotating coating process under an applied magnetic field. Section 3 presents the stability analysis for coating modeling for standard approaches using long-wave perturbation techniques, the multiple scales method and the Ginzburg-Landau equation. Section 4 presents several numerical examples to illustrate the effectiveness of the proposed method.

GENERALIZED MATHEMATICAL FORMULATION

Consider the axisymmetric flow of an electrically conductive polymer resist film designated as a power low model flowing on a vertical rotating coating process with a constant angular velocity Ω^* under an applied magnetic field. The external uniform magnetic field is applied perpendicular to the plane of the vertical cylinder (see Fig. 1).

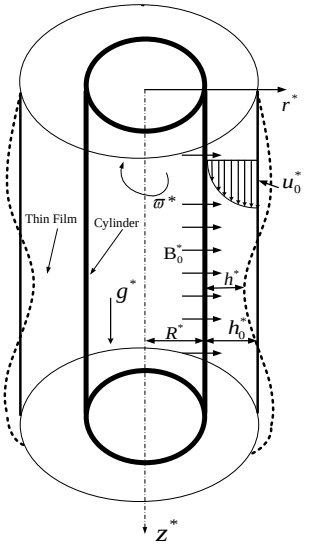

Fig. 1 Schematic diagram of a general viscous magnetic fluid film flow traveling along a rotating vertical cylinder

This model entails certain assumptions including: (1) the film flow is rotationally symmetrical, (2) the film flow velocity is independent of θ^* and there is a negligible circumferential flow given a very thin physical coating flow ($h^* << r^*$), And (3) due to the lack of phase change effects, all associated physical properties are assumed to be constant (i.e. time-invariant). A variable with a superscript "*" represents a dimensional quantity. u^* and w^* are respectively the velocity components in the cylinder's radial direction r^* and the perpendicular direction z^*. For the sake of simplicity, the only applied magnetic field is B_0^* when the imposed and induced electric fields are negligible at a magnetic Reynolds number much less than 1. The electromagnetic force is $\sigma^* B_0^* w^*$ (Attia, 1998; Hayat, Javed & Sajid, 2008). The flow couples the Navier-Stokes equations and Maxwell's equations for the magnetic field on a vertical rotating coating process. The governing equations of continuity and motion are as follows (Cheng & Chu, 2009)

$$\frac{1}{r^*}\frac{\partial(r^* u^*)}{\partial r^*}+\frac{\partial w^*}{\partial z^*}=0 \tag{1}$$

$$\begin{aligned}&\rho^*\left(\frac{\partial u^*}{\partial t^*}+u^*\frac{\partial u^*}{\partial r^*}+w^*\frac{\partial u^*}{\partial z^*}-\frac{v^{*2}}{r^*}\right)\\&=\frac{1}{r^*}\frac{\partial(r^*\tau_{r^*r^*})}{\partial r^*}+\frac{\partial\tau_{z^*r^*}}{\partial z^*}-\frac{1}{r^*}\tau_{\theta^*\theta^*}\end{aligned} \tag{2}$$

$$\begin{aligned}&\rho^*\left(\frac{\partial w^*}{\partial t^*}+u^*\frac{\partial w^*}{\partial r^*}+w^*\frac{\partial w^*}{\partial z^*}\right)\\&=\frac{1}{r^*}\frac{\partial(r^*\tau_{r^*z^*})}{\partial r^*}+\frac{\partial\tau_{z^*z^*}}{\partial z^*}+\rho^* g^*-\sigma^* B_0^{*2} w^*\end{aligned} \tag{3}$$

where v^* is tangential velocity, ρ^* is constant fluid density, p^* is fluid pressure, g* is acceleration due to gravity and the individual stress components are given as (Lin, 2014)

$$\tau^*_{r^*r^*}=-p^*+2\mu_n^*\left(\frac{\partial u^*}{\partial r^*}\right)^n \tag{4}$$

$$\tau^*_{z^*z^*}=-p^*+2\mu_n^*\left(\frac{\partial w^*}{\partial z^*}\right)^n \tag{5}$$

$$\tau^*_{r^*z^*}=\tau^*_{z^*r^*}=\mu_n^*\left(\frac{\partial u^*}{\partial z^*}+\frac{\partial w^*}{\partial r^*}\right)^n \tag{6}$$

$$\tau^{*}{}_{\theta^*\theta^*} = -p^{*} + 2\mu_n^{*}\left(\frac{u^{*}}{r^{*}}\right)^{n} \tag{7}$$

where n is the flow index of the power law model and μ_n^{*} is the fluid dynamic viscosity of the polymer resists. On the surface of the vertical cylinder at $r^{*} = R^{*}$, and the boundary conditions are treated as no-slip as follows

$$u^{*} = 0 \tag{8}$$

$$w^{*} = 0 \tag{9}$$

On the free surface $r^{*} = R^{*} + h^{*}$, and the boundary condition approximated by the vanishing of shear stress is given as

$$\begin{aligned}&\frac{\partial h^{*}}{\partial z^{*}}\left[1+\left(\frac{\partial h^{*}}{\partial z^{*}}\right)^{2}\right]^{-1}\left(\tau_{r^*r^*} - \tau_{z^*z^*}\right)\\ &+\left[1-\left(\frac{\partial h^{*}}{\partial z^{*}}\right)^{2}\right]\left[1+\left(\frac{\partial h^{*}}{\partial z^{*}}\right)^{2}\right]^{-1}\tau_{r^*z^*} = 0\end{aligned} \tag{10}$$

By solving the balance equation in the direction normal to the free surface, the resulting normal stress condition can be expressed as

$$\begin{aligned}&\left[1+\left(\frac{\partial h^{*}}{\partial z^{*}}\right)^{2}\right]^{-1}\left[2\tau_{r^*z^*}\frac{\partial h^{*}}{\partial z^{*}} - \tau_{r^*r^*} - \tau_{z^*z^*}\left(\frac{\partial h^{*}}{\partial z^{*}}\right)^{2}\right]\\ &+S^{*}\left\{\frac{\partial^{2} h^{*}}{\partial z^{*2}}\left[1+\left(\frac{\partial h^{*}}{\partial z^{*}}\right)^{2}\right]^{-3/2} - \frac{1}{r^{*}}\left[1+\left(\frac{\partial h^{*}}{\partial z^{*}}\right)^{2}\right]^{-1/2}\right\}\\ &+\frac{k^{*2}(\zeta-1)}{\rho^{*}\zeta h_{fg}^{*2}}\left[1+\left(\frac{\partial h^{*}}{\partial z^{*}}\right)^{2}\right]^{-1}\left(\frac{\partial T^{*}}{\partial r^{*}} - \frac{\partial T^{*}}{\partial z^{*}}\frac{\partial h^{*}}{\partial z^{*}}\right)^{2} = p_g^{*}\end{aligned} \tag{11}$$

The kinematic condition that ensures the flow does not travel across a free surface, it follows that

$$\frac{\partial h^{*}}{\partial t^{*}} + \frac{\partial h^{*}}{\partial z^{*}}w^{*} - u^{*} = 0 \tag{12}$$

where h^{*} is the local film thickness, S_n^{*} is the surface tension and p_a^{*} is the atmospheric pressure. By introducing a stream function φ^{*}, the dimensional velocity components become

$$u^{*} = \frac{1}{r^{*}}\frac{\partial \varphi^{*}}{\partial z^{*}}, \quad w^{*} = -\frac{1}{r^{*}}\frac{\partial \varphi^{*}}{\partial r^{*}} \tag{13}$$

The following dimensionless quantities are used to form the dimensionless governing equations and boundary conditions

$$r = \frac{r^{*}}{h_0^{*}}, \quad z = \frac{\alpha z^{*}}{h_0^{*}}, \quad t = \frac{\alpha u_0^{*} t^{*}}{h_0^{*}}, \quad h = \frac{h^{*}}{h_0^{*}},$$

$$\varphi = \frac{\varphi^{*}}{u_0^{*} h_0^{*2}}, \quad p = \frac{p^{*} - p_a^{*}}{\rho u_0^{*2}}, \quad \mathrm{Re}_n = \frac{u_0^{*2-n} h_0^{*n}}{\nu_n},$$

$$\alpha = \frac{2\pi h_0^{*}}{\lambda^{*}}, \quad S_n = \frac{S_n^{*}}{\left(2^{-3n^2+3n+2}\rho_n^{n+2}\nu_n^{4} g^{3n-2}\right)^{\frac{1}{n+2}}} \tag{14}$$

where h_0^{*} is the average film thickness, α is the dimensionless wave number, ν_n^{*} is the kinematic viscosity, Re_n^{*} is the Reynolds number, S_n^{*} is the dimensionless surface tension, m is the Hartmann number, λ is the wavelength, and u_0^{*} is the scale of velocity defined as

$$u_0^{*} = \frac{1}{4}\left(\frac{g^{*}}{\nu_n^{*}}\right)^{\theta}\frac{h_0^{*1+\theta}}{\Gamma} \tag{15}$$

where

$$\theta = 1/n, \tag{16}$$

$$\Gamma = \left[2(1+R)^{2}\ln\left(\frac{1+R}{R}\right) - (1+2R)\right]^{-1} \quad (n=1) \tag{17}$$

$$\Gamma = \frac{2^{-2+\theta}(-2+\theta)(-1+\theta)R^{\theta}(1+R)^{\theta}(1+2R)^{1-\theta}}{-R(1+R)^{\theta}\{2+4R+\theta[-1+2(R-1)R]\} + R^{\theta}(1+R)\{2+4R+\theta[-1+2R(\theta-2+R)]\}} \quad (n\neq 1) \tag{18}$$

To investigate the effects of angular velocity, Ω^{*}, on the coating flow stability, the dimensionless Rossby number, β, and the Hartmann number, m , are defined as

$$\beta = \frac{\Omega^{*} h_0^{*}}{u_0^{*}}, \quad m = \left(\frac{\sigma^{*} B_0^{*2} h_0^{*2}}{\rho^{*}\nu_n^{*}}\right)^{1/2} \tag{19}$$

For these non-dimensional variables, the governing equations can be expressed as

$$\begin{aligned}\frac{\partial p}{\partial r} = \alpha\cdot\mathrm{Re}_n^{-1}\{&n[2(\frac{\partial}{\partial r}(\frac{1}{r}\frac{\partial\varphi}{\partial z}))^{n-1}\frac{\partial^2}{\partial r^2}(\frac{1}{r}\frac{\partial\varphi}{\partial z}) - (\frac{\partial}{\partial r}(\frac{1}{r}\frac{\partial\varphi}{\partial r}))^{n-1}\frac{\partial^2}{\partial r\partial z}(\frac{1}{r}\frac{\partial\varphi}{\partial r})]\\ &+\frac{2}{r}[(\frac{\partial}{\partial r}(\frac{1}{r}\frac{\partial\varphi}{\partial z}))^{n} - (\frac{1}{r^2}\frac{\partial\varphi}{\partial z})^{n}]\} + \frac{(R\beta)^2}{r} + O(\alpha^2)\end{aligned} \tag{20}$$

$$\begin{aligned}&\frac{1}{r}\frac{\partial}{\partial r}\{r[\frac{\partial}{\partial r}(\frac{1}{r}\frac{\partial\varphi}{\partial r})]^{n}\} - (4\Gamma)^{n-1}\frac{m}{r}\frac{\partial\varphi}{\partial r} = (4\Gamma)^{n}\\ &+\alpha\,\mathrm{Re}_n[-\frac{\partial p}{\partial z} + \frac{1}{r}\frac{\partial^2\varphi}{\partial t\partial r} + \frac{1}{r^2}\frac{\partial\varphi}{\partial z}\frac{\partial^2\varphi}{\partial r^2} - \frac{1}{r^3}\frac{\partial\varphi}{\partial z}\frac{\partial\varphi}{\partial r} - \frac{1}{r^2}\frac{\partial\varphi}{\partial r}\frac{\partial^2\varphi}{\partial r\partial z}] + O(\alpha^2)\end{aligned} \tag{21}$$

Using the non-dimensional variables, the boundary conditions at the cylinder surface $(r = R)$ are reduced to

$$\varphi = \varphi_r = \varphi_z = 0 \tag{22}$$

and the boundary conditions at the free surface of the cylinder $(r = R + h)$ become

$$\frac{\partial}{\partial r}\left(\frac{1}{r}\frac{\partial\varphi}{\partial r}\right) = 0 + O(\alpha^2) \tag{23}$$

$$p = -2S_n\cdot\mathrm{R}_n^{\frac{-3n^2+4n+4}{(n+2)(n-2)}}(2\Gamma)^{\frac{(3n-2)n}{n+2}}\left(\alpha^2\frac{\partial^2 h}{\partial z^2} - \frac{1}{r}\right)$$

$$+\alpha\frac{2}{\mathrm{R}_{\beta}}[\{\frac{\partial}{\partial r}(\frac{1}{r}\frac{\partial\varphi}{\partial r})\}\frac{\partial h}{\partial z}+(\frac{\partial}{\partial r}(\frac{1}{r}\frac{\partial\varphi}{\partial z})\}]+O(\alpha^2) \quad (24)$$

$$\frac{\partial h}{\partial t}-\frac{1}{r}(\frac{\partial\varphi}{\partial r}\frac{\partial h}{\partial z}+\frac{\partial\varphi}{\partial z})=0 \quad (25)$$

Hence the term α^2 S can be treated as a quantity of the zeroth order (Lin, 2012; Lin, 2014). We use long-wave perturbation techniques (Benney, 1974) by expanding the stream function and flow pressure in terms of some small wave number ($\alpha<<1$) as

$$\varphi=\varphi_0+\alpha\varphi_1+O(\alpha^2) \quad (26)$$

$$p=p_0+\alpha p_1+O(\alpha^2) \quad (27)$$

We can obtain the coating film flow conditions by inserting the above expressions into equations (20)-(25) and then systematically solving the resulting equations. The solutions of the zeroth order and first order equations were obtained and are given in Appendix A. The zeroth and first order solutions are inserted into the dimensionless free surface kinematic equation to yield the following generalized nonlinear kinematic equation

$$h_t+A(h)h_z+B(h)h_{zz}+C(h)h_{zzzz}+D(h)h_z^2+E(h)h_zh_{zzz}=0 \quad (28)$$

where $A(h)$, $B(h)$, $C(h)$, $D(h)$ and $E(h)$ are given in Appendix B.

STABILITY ANALYSIS

Some perturbations are unavoidable in any coating process, thus we study the stability of a steady state undisturbed liquid film. The thickness of the dimensionless film can be expressed in terms of the perturbation variables as

$$h(t,z)=1+\eta(t,z),\qquad \eta=O(\alpha) \quad (29)$$

where η is the perturbed quantity of the stationary coating thickness. The value of $h(r,t)$ is substituted into generalized nonlinear kinematic equation (28) and all terms up to order η^3 are collected. The evolution equation of η is obtained as

$$\begin{aligned}&\eta_t+X'\eta_Z+A\eta_z+B\eta_{zz}+C\eta_{zzzz}\\&=-[(\frac{X''}{2}\eta^2+\frac{X'''}{6}\eta^3)+(A'\eta+\frac{A''}{2}\eta^2)\eta_z+(B'\eta+\frac{B''}{2}\eta^2)\eta_{zz}\\&+(C'\eta+\frac{C''}{2}\eta^2)\eta_{zzzz}+(D+D'\eta)\eta+(E+E'\eta)\eta_z\eta_{zzz}]+O(\eta^4)\end{aligned} \quad (30)$$

where the values of A~E and their corresponding derivatives are all evaluated in terms of the dimensionless height of the film h=1.

Linearized stability analysis

The effect of perturbation on coating flow instability is of particular interest and the perturbation behavior can assume various forms. The present analysis begins with linearized analysis. When the nonlinear terms of equation (30) are neglected, the linearized equation is given as

$$\eta_t+A\eta_z+B\eta_{zz}+C\eta_{zzzz}=0 \quad (31)$$

To use the normal mode analysis, we assume that

$$\eta=a\exp[i(z-dt)]+c.c. \quad (32)$$

where a is the small perturbation amplitude, and c.c. is its complex conjugate counterpart. The complex wave celerity, d is given as

$$d=d_r+id_i=A+i(B-C) \quad (33)$$

where d_r and d_i are respectively the linear wave speed and linear growth rate of the disturbance. The solution of the disturbance about $h(r,t)$ =1 is asymptic stability or instability depending on whether $d_i<0$ or $d_i>0$.

Weak stability effects

To derive the nonlinear behaviors of the thin film flows, we use the same procedure (Cheng et al., 2009; Lin, 2012) and apply the multiple scales method (Krishna & Lin, 1977)

$$\frac{\partial}{\partial t}\rightarrow\frac{\partial}{\partial t}+\varepsilon\frac{\partial}{\partial t_1}+\varepsilon^2\frac{\partial}{\partial t_2} \quad (34)$$

$$\frac{\partial}{\partial r}\rightarrow\frac{\partial}{\partial r}+\varepsilon\frac{\partial}{\partial r_1} \quad (35)$$

$$\eta(\varepsilon,r,r_1,t,t_1,t_2)=\varepsilon\eta_1+\varepsilon^2\eta_2+\varepsilon^3\eta_3 \quad (36)$$

where ε is a small perturbation parameter, slow scales $t_1=\varepsilon t$, $r_1=\varepsilon r$, the additional time scale $t_2=\varepsilon^2 t$ Then, equation (30) becomes

$$(L_0+\varepsilon L_1+\varepsilon^2L_2)(\varepsilon\eta_1+\varepsilon^2\eta_2+\varepsilon^3\eta_3)=-\varepsilon^2N_2-\varepsilon^3N_3 \quad (37)$$

(nonlinear terms)

Where

$$L_0=\frac{\partial}{\partial t}+X'+A\frac{\partial}{\partial r}+B\frac{\partial}{\partial r^2}+C\frac{\partial}{\partial r^3}+D\frac{\partial}{\partial r^4} \quad (38)$$

$$L_1=\frac{\partial}{\partial t_1}+A\frac{\partial}{\partial r_1}+2B\frac{\partial}{\partial r}\frac{\partial}{\partial r_1}+3C\frac{\partial^2}{\partial r^2}\frac{\partial}{\partial r_1}+4D\frac{\partial^3}{\partial r^3}\frac{\partial}{\partial r_1} \quad (39)$$

$$L_2=\frac{\partial}{\partial t_2}+B\frac{\partial^2}{\partial r_1^2}+3C\frac{\partial}{\partial r}\frac{\partial^2}{\partial r_1^2}+6D\frac{\partial^2}{\partial r^2}\frac{\partial^2}{\partial r_1^2} \quad (40)$$

$$N_2=\frac{X''}{2}\eta_1^2+A'\eta_1\eta_{1r}+B'\eta_1\eta_{1rr}+C'\eta_1\eta_{1rrr}+D'\eta_1\eta_{1rrr}+E\eta_{1r}^2+F\eta_{1r}\eta_{1rrr} \quad (41)$$

$$N_3 = X^{"}\eta_1\eta_2 + A^{'}(\eta_1\eta_{2r} + \eta_{1r}\eta_2 + \eta_1\eta_{1r_{\eta_1}}) + B^{'}(\eta_1\eta_{2rr} + 2\eta_1\eta_{1rr_{\eta_1}} + \eta_{1rr}\eta_2)$$
$$+ C^{'}(\eta_1\eta_{2rrr} + 3\eta_1\eta_{1rrr_{\eta_1}} + \eta_{1rrr}\eta_2) + D^{'}(\eta_1\eta_{2rrr} + 4\eta_1\eta_{1rrr_{\eta_1}} + \eta_{1rrr}\eta_2)$$
$$+ E(2\eta_{1r}\eta_{2r} + 2\eta_{1r}\eta_{1r_{\eta_1}}) + F(\eta_{1r}\eta_{2rrr} + 3\eta_{1r}\eta_{1rrr_{\eta_1}} + \eta_{1rrr}\eta_{2r} + \eta_{1rrr}\eta_{1r_{\eta_1}}) + \frac{1}{6}X^{'''}\eta_1^3 + \frac{1}{2}A^{"}\eta_1^2\eta_{1r}$$
$$+ \frac{1}{2}B^{"}\eta_1^2\eta_{1rr} + \frac{1}{2}C^{"}\eta_1^2\eta_{1rrr} + \frac{1}{2}D^{"}\eta^2{}_1\eta_{1rrr} + E^{'}\eta_1\eta_{1r}{}^2 + F^{'}\eta_1\eta_{1r}\eta_{1rrr} \quad (42)$$

Equation (37) is solved order by order. After collecting the order $O(\varepsilon)$ and solving for the equation $L_0\eta_1 = 0$, the solution of η_1 is

$$\eta_1 = a(r_1 - c_r, t_1, t_2)\exp[i(r - d_r t)] + c.c. \quad (43)$$

After collecting the order $O(\varepsilon^2)$ and solving for the secular equation, the solution of η_2 is

$$\eta_2 = ea^2\exp[2i(r - d_r t)] + c.c. \quad (44)$$

By plugging both η_1 and η_2 into the equation of order $O(\varepsilon^3)$,the Ginzburg–Landau equation (Ginzburg & Landau, 1950) is given as

$$\frac{\partial a}{\partial t_2} + D_1\frac{\partial^2 a}{\partial r_1^2} - \varepsilon^{-2}d_i a + (E_1 + iF_1)a^2\bar{a} = 0 \quad (45)$$

where

$$e = e_r + ie_i = (B^{'} - C^{'} + D - E)/(16C - 4B) + iA^{'}/(4B - 16C) \quad (46)$$

$$D_1 = B - 6C \quad (47)$$

$$E_1 = (-5B^{'} + 17C^{'} + 4D - 10E)e_r - A^{'}e_i + (-3B^{"}/2 + 3C^{"}/2 + D^{'} - E^{'}) \quad (48)$$

$$F_1 = (-5B^{'} + 17C^{'} + 4D - 10E)e_i + A^{'}e_r + A^{"}/2 \quad (49)$$

The overhead bar in Eq. (45) represents the complex conjugate of the same variable. Equation (45) can be used to assess the weak nonlinear behavior of the fluid film flow. To solve for Eq. (45), we assume a filtered wave with no spatial modulation, so the filtered wave can be expressed as

$$a = a_0\exp[-ib(t_2)t_2] \quad (50)$$

After substituting Eq. (50) into Eq.(45), we obtain

$$\frac{\partial a_0}{\partial t_2} = (\varepsilon^{-2}d_i - E_1 a_0^2)a_0 \quad (51)$$

$$\frac{\partial[b(t_2)t_2]}{\partial t_2} = F_1 a_0^2 \quad (52)$$

The associated wave amplitude εa_0 in the supercritical stable region is derived and given as

$$\varepsilon a_0 = \sqrt{\frac{d_i}{E_1}} \quad (53)$$

$$Nc_r = d_r + d_i\left(\frac{F_1}{E_1}\right) \quad (54)$$

If $E_1 = 0$, then Eq. (51) is reduced to a linear equation. The second term on the right-hand side of Eq. (51) results from nonlinearity and may moderate or accelerate the exponential growth of the linear disturbance according to d_i and E_1. Equation (51) modifies the perturbed wave speed caused by infinitesimal disturbances in the nonlinear system. The Ginzburg–Landau equation can be used to characterize various flow states.

NUMERICAL EXAMPLES

To demonstrate the effectiveness of the proposed mathematical models, numerical examples are presented to verify the solutions. The general viscous fluid considered in the present study represents the rate of deformation, and should be designated as a "power-law model" (valid only for high shear rate regions such as those in polymer process models). In fact, a power-law model represents each polymer resist film as unique, requiring the direct evaluation of its rheological behavior. The practical fluid used here (Chhabra et al., 2008) includes a certain mixture of polymethyl methacrylate in pyridine with a density ρ=0.98 x 103 kg/m3 and a fluid dynamic viscosity μn =0.79 N s/m2 to create a film with thickness of the order $h_0^* = 10^{-2}m$. The physical parameters and the range of their values for the numerical experiments are based on previous findings (Lin, 2014). To study the effects of magnetohynamic forces, rotational motion and flow index on coating flow stability, we performed numerical experiments using randomly selected physical parameters within specified ranges based on previous works (Lin, 2014; Cheng et al., 2009), including: (1) Reynolds number (0 to 10); (2) dimensionless perturbation wave numbers (0 to 0.12); (3) Hartmann number (0, 0.1 or 0.2) ; (4) Rossby number (0.1 or 0.2) and (5) flow index (0.95, 1, or 1.05). The remaining parameters are treated as constants for all numerical computations. Furthermore, to simplify the analysis, the dimensionless surface tension S=6173.5 and the dimensionless radius R=20.

Weakly nonlinear stability analysis

The effects of rotation number and cylinder size on the film flow linear stability are well established (Chen et al. 2004; Chen et al. 2005). This paper studies the weakly nonlinear effects of the evolution equation with consideration of many potential mechanisms including centrifugal forces, magnetohynamic forces, inertia and film viscous stress. Figures 2(a) to (d) show various conditions for sub-critical instability $(d_i < 0, E_1 < 0)$, sub-critical stability $(d_i < 0, E_1 > 0)$, supercritical stability $(d_i > 0, E_1 > 0)$ and the supercritical explosion $(d_i > 0, E_1 < 0)$.

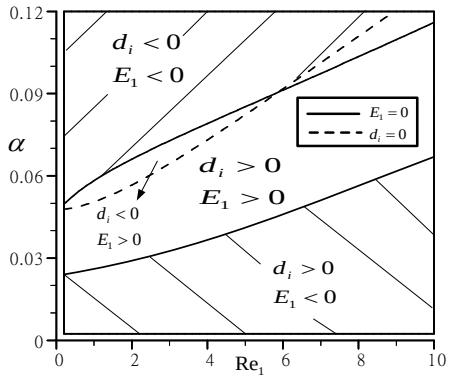

Fig. 2(a) Neutral stability curves for m=0.1, β =0.1, n=0.95, and R=20

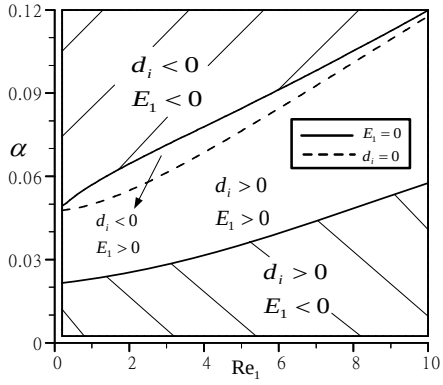

Fig. 2(b) Neutral stability curves for m=0.2, β =0.1, n=0.95, and R=20

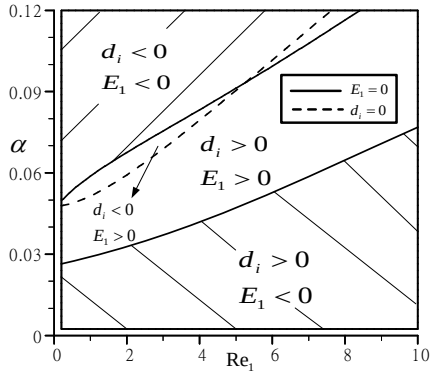

Fig. 2(c) Neutral stability curves for m=0.1, β =0.2, n=0.95, and R=20

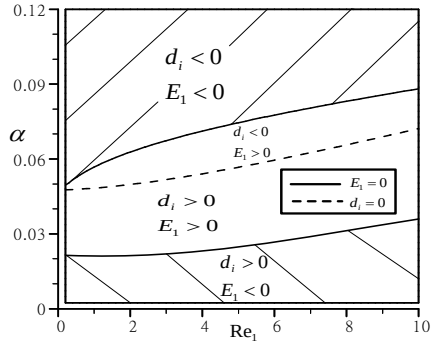

Fig. 2(d) Neutral stability curves for m=0.1, β =0.1, n=1.05, and R=20

Figure 3(a) shows the threshold amplitude in the sub-critical instability region for various wave numbers with different m values at Re1=5, R=20, n=0.95, and β =0.1. The results show that the threshold amplitude εa_0 decreases with the Hartmann number (m) value due to the magnetohynamic forces, en external force in the governing equation. Increasing the Hartmann number can inhibit the growth of the linear disturbance due to the Lorentz forces, thereby contributing to flow stabilization. Figure 3(b) shows the threshold amplitude in the sub-critical instability region for various wave numbers with different n values at Re1=4, R=20, m=0.2 and β =0.1. The results show that the threshold amplitude εa_0 decreases with the flow index (n) value because of the viscous stresses term, an internal force in the governing equation. The microstructure characteristic of a polymer resists dissipates the energy of the linear disturbance due to effective viscosity increasing with n and thus contributing to flow stabilization.

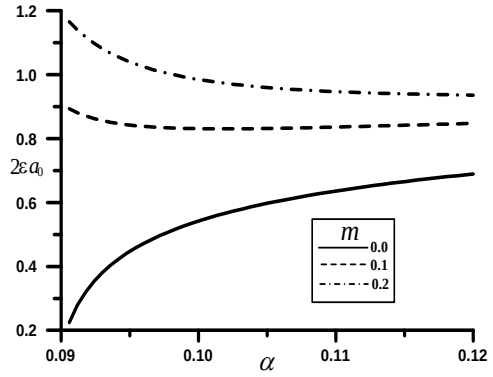

Fig. 3(a) Threshold amplitude in subcritical unstable region for three different values of m. Note that Re_1=5, R=20, n=0.95, and $\beta = 0.1$

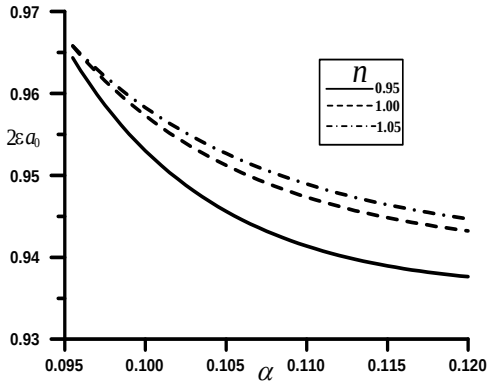

Fig. 3(b) Threshold amplitude in subcritical unstable region for three different values of n. Note that Re_1=4, R=20, β =0.1, and m=0.2

Figure 4(a) shows the threshold amplitude in the supercritical stability region for various wave

numbers with different m values at Re_1=4, β=0.1, n=0.95, and R=20. Increasing the m value decreases the maximum threshold amplitude. Figure 4(b) shows the nonlinear wave speed in the supercritical stable region for various wave numbers with different m values for the same film flow. The nonlinear wave speed is inversely correlated to the m value . Figure 4(c) shows the threshold amplitude in the supercritical stability region for various wave numbers with different n values at Re_1=6, m=0.2, β =0.1, and R=20. The n is inversely correlated to the maximum threshold amplitude. Figure 4(d) shows the nonlinear wave speed in the supercritical stable region for various wave numbers with different n values for the same film flow. The nonlinear wave speed is inversely correlated to the n value. In the above cases, the wave amplitudes fluctuate with the nonlinear terms resulting in energy transfers between different waves, thus changing their amplitudes.

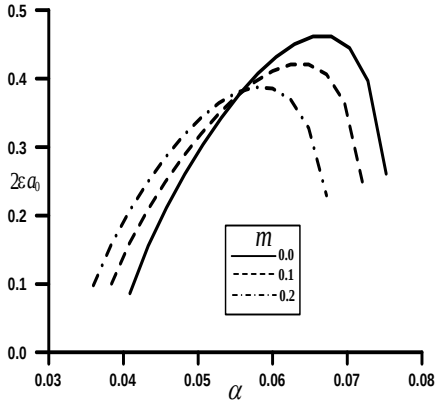

Fig. 4(a) Threshold amplitude in supercritical stable region for three different values of m. Note that Re_1=4, β=0.1, n=0.95, and R=20

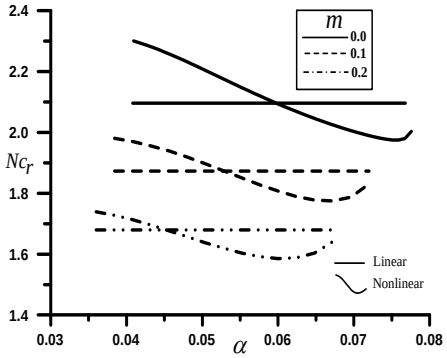

Fig. 4 (b) Nonlinear wave speed in supercritical stable region for three different values of m. Note that Re_1=4, β=0.1, n=0.95, and R=20

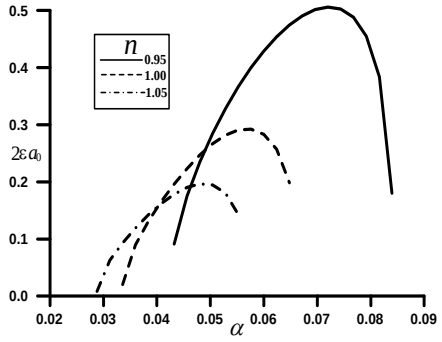

Fig. 4(c) Threshold amplitude in supercritical stable region for three different values of n. Note that Re_1=6, m=0.2, β=0.1, and R=20

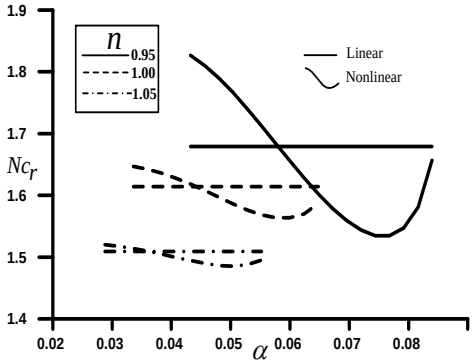

Fig. 4(d) Nonlinear wave speed in supercritical stable region for three different values of n. Note that Re_1=6, m=0.2, β=0.1, and R=20

CONCLUDING REMARKS

To simplify analysis and computations, a number of assumptions are made regarding the flow of matter: (1) the dimensions of the general viscous fluid consistency coefficient are assumed to depend on the numerical value of the flow index n. (2) The present study is limited to the higher shear rate region (i.e., n approaching 1). Based on numerical modeling results, several conclusions can be drawn as follows.

1. Due to t the viscous stresses term, the microstructure characteristics of a polymer resist dissipate the energy of a linear disturbance due to the effective viscosity increasing with n, thus contributing to film flow stabilization with the rotation effect due to centrifugal forces.
2. Material flows as dilatant fluid are more stable than pseudo plastic fluid with the same coating flow.
3. Enhancing the magnetic effects enhances the stabilization of the polymer resist films as general viscous fluids using a spin cylinder at a low Reynolds number due to the Lorentz forces.
4. Using appropriate operating conditions such as a low Reynolds number (Re1<6) or a slow rotation effects (β <0.2), the necessary conditions of the

various critical flow states can be determined by the Ginzburg-Landau equation in practical polymer resist films.

REFERENCES

Acrivos, A., Shah, M. J., Petersen, E. E. (1960). On the flow of a non-Newtonian liquid on a rotating disk. J. Appl. Phys, 31 (6) 963-968.

Agassi, Y. D. (2015). AC losses in superconductors with a power-law constitutive relation. Physica C, 517, 41-48.

Attia, H.A. (1998). Unsteady MHD flow near a rotating porous disk with uniform suction or injection. Fluid Dyn. Res., 23, 283-290.

Benney, D. J. (1974). Long waves on liquid films. J. Fluid Mech, 63, 417-429.

Burgess, S. L., Wilson, S. D. R. (1996). Spin-coating of a viscoplastic material. Phys. Fluids, 8, 2291-2297.

Chen, C. I., Chen, C. K.,Yang, Y. T. (2004). Perturbation Analysis to the Nonlinear Stability Characterization of the Thin Condensate Falling Film on the Outer Surface of a Rotating Vertical Cylinder. Int. J. Heat Mass Tran, 47, 1937-1951.

Chen C. I., Chen, C. K., Yang, Y. T. (2005). Nonlinear-stability analysis of a thin Newtonian film flowing down an infinite vertical rotating cylinder. P. I. Mech. Eng. C-J Mec, 219, 911-923.

Cheng, P. J., Chu, I. P. (2009). Nonlinear hydromagnetic stability analysis of a pseudoplastic film flow. Aerosp. Sci. Technol., 13, 247-255.

Chhabra, R. P., Richardson, J. F. (2008). Non-Newtonian flow and applied rheology: engineering applications. Butterworth-Heinemann. U.K.

Cipolatti, R., Dickstein, F., Puel, J. P. (2015). Existence of standing waves for the complex Ginzburg–Landau equation. J. Math. Anal. Appl, 422, 579–593.

Garmroodi, M. R., Ahmadpour, A., Talati, F. (2019). MHD mixed convection of nanofluids in the presence of multiple rotating cylinders in different configurations: A two-phase numerical study. Int. J. Mech. Sci, 150, 247-264.

Ginzburg, V. L., Landau, L. D. (1950). Theory of Superconductivity. J. of Exp. Theor. Phys(USSR), 20, 1064-1082.

Hayat, T., Javed, T., Sajid, M. (2008). Analytic solution for MHD rotating flow of a second grade fluid over a shrinking surface. Phys. Letters A, 372, 3264-3273.

Jiang, W., Shen, L., Xu, M., Wang, Z., Tian, Z. (2019). Mechanical properties and corrosion resistance of Ni-Co-SiC composite coatings by magnetic field-induced jet electrodeposition. J. Alloys Compd, 791, 847-855.

Khan, Z., Islam, S., Shah, R. A., Khan, M. A., Bonyah, E., Jan, B., Khan, A. (2017). Double-layer optical fiber coating analysis in MHD flow of an elastico-viscous fluid using wet-on-wet coating process. Results Phys., 7, 107-118.

Kozitskiy, S. B. (2020). The first 180 Lyapunov exponents for two-dimensional complex Ginzburg-Landau-type equation. Commun. Nonlinear Sci, 84, 105172.

Krishna, M. V. G., Lin, S. P. (1977). Nonlinear Stability of a Viscous Film with Respect to Three-dimensional Side-band disturbance. Phys. Fluids, 20, 1039-1044.

Lin, M. C. (2012). Long-wave perturbation analysis to the stability of a thin viscoplastic material flowing on a rotating circular disk. Int. J. Eng, 53, 112-123.

Lin, M. C. (2014). Surface instability of thin polymer resist films with phase change effects on coating flow using numerical approximation techniques. Comput. Math. with Appl., 68, 847-858.

Liu, Y. L., Chen, S. Y., Wang, K. S. (2009). Polymeric spheres on substrates from a spin-coating process. J. of Colloid and Interface Sci, 330, 73-76.

Mahmood, R., Bilal, S., Majeed, A. H., Khan, I., Sherif, M. (In press 2019). A comparative analysis of flow features of Newtonian and power law material: A New configuration. J. Mater. Res. Technol.

Perez, L. M., Laroze, D., Diaz, P., Martines-Mardones, J., Mancini, H. L. (2014). Rotating convection in a viscoelastic magnetic fluid. J. Magn. Magn. Mater, 364, 98-105.

Sadigh, M. A., Paygozar B., Silva, L.F.M., VakiliTahami, F. (2019). Creep deformation simulation of adhesively bonded joints at different temperature levels using a modified power-law model. Polym. Test, 79, 106087.

Schewe, G. (2013). Flow-induced vibrations and the Landau equation. J. Fluid Struct, 43, 256–270.

Singh, K. D. (2000). An oscillatory hydromagnetic coquette flow in a rotating system. Math. Mech., 80, 429-432.

VeeraKrishna, M., Sravanthi, C. S., ReddyGorla, R. S. (2020). Hall and ion slip effects on MHD rotating flow of ciliary propulsion of microscopic organism through porous media. Int. Commun. Heat Mass, 112, 104500.

Xu, P., Zou, G., Huang, J. (2019). time–space fractional stochastic Ginzburg–Landau equation driven by fractional Brownian motion. Comput. math. with Appl, 78, 3790-3806.

Yıldırım,Y., Biswas, A., Jawad, A. J. M., Ekici, M., Zhouh, Qin, Alzahrani, A. K., Belic, M. R. (2020). Optical solitons with differential group delay for complex Ginzburg–Landau equation. Results Phys, 16, 102888.

Zou, L., Håkansson, U., Cvetkovic, V. (2020). Yield-power-law fluid propagation in water-saturated fracture networks with application to rock grouting.Tunn. Undergr. Sp. Tech, 95,103170.

APPENDIX A

Zeroth-ordersolution:

$$\varphi_0 = n(4\Gamma)^n (r-R)^2\{60nhR^2(h-2R)-20(r-R)R\Phi/n+5(r-R)^2[4nR^2 +3h^2(n+mR^2)-2hR(n+mR^2)]-8(r-R)^3[nR+h(n+mR^2)]\}/(120\Omega) \quad (A.1)$$

where

$$\Phi = 2nR^2 - 4nhR + (3n+mR^2)h^2 \quad (A.2)$$

$$\Omega = 2nR^2 - 2nhR + (2n+mR^2)h^2$$

and

$$\varphi_1 = k_2(r-R)^2 + k_3(r-R)^3 + k_4(r-R)^4 + k_5(r-R)^5 \quad (A.3)$$

where

$$k_2 = \xi hR^2(2R-h)(h_z+\alpha^2 q h_{zzz})/(q^2\Omega) + \mathrm{Re}\,\beta^2 h_z h(h-2R)R^4/(2q\Omega) \quad (A.4)$$

$$k_3 = \xi R\Phi(h_z+\alpha^2 q h_{zzz})/(q^2\Omega) + 4^n\,\mathrm{Re}_n R^4\Gamma^n h[R^2 h(3n+mR^2)+8nR^3+2n+2mR^2] h_{0t}/(2\Omega^3) + \mathrm{Re}\,\beta^2 h_z R^3\Phi/(6nq\Omega) \quad (A.5)$$

$$k_4 = -\mathrm{Re}_n R^5\Gamma^{-2n} h^2 h_z\{16^n h[16nR^3+(n+mR^2)h^3]+2\cdot 16^n R[4nR^3+h^2(3nR -2mR^3+(n+2mR^2)h)]\}/(2\Omega^4) + \xi[4nR^2+h(n+mR^2)](-2R+3h) (h_z+\alpha^2 q h_{zzz})/(12nq^2\Omega) - 4^n R^3\Gamma^n\Omega h_{0t}[4nR^2-2nRh+(3n+2mR^2)h^2] [2nR^2-2nhR+(n+mR^2)h^2]/(6n\Omega^4) + \mathrm{Re}\beta^2 h_z R^2[4nR^2+h(3h-2R) (n+mR^2)]/(24nq\Omega) \quad (A.6)$$

$$k_5 = 16^n\,\mathrm{Re}_n hh_z R^4\Gamma^{-2n}(2R-h)[2nhR-2nR^2+(n+mR^2)h^2]/(6n\Omega^2) - 2\xi[nR +(n+mR^2)h](h_z+\alpha^2 q h_{zzz})/(15nq^2\Omega) + 4^n R^2\Gamma^n h_{0t}[h(3n+mR^2)/2+4nR^3 +(n+mR^2)h^3]/(12n\Omega^3) + \mathrm{Re}\,\beta^2 h_z R^2[n(R+h)+hmR^2)]/(15nq\Omega) \quad (A.7)$$

where

$$q = R+h,\quad \xi = S_n\,\mathrm{Re}_n^{\frac{-2n}{n+2}}(2\Gamma)^{\frac{(3n-2)n}{2+n}},\quad h_{0t} = r^{-1}(\varphi_{0r}h_z+\varphi_{0z}) \quad (A.8)$$

Appendix B

$$A(h) = -4^{n-1}h^2\Gamma^n[160n^2hR^4-240n^2R^5+2nh^3R^2(-63n+mR^2)+14h^5(n+mR^2) (2n+mR^2)+10h^2R^3(13n+mR^2)+h^4(91n^2R+58nmR^3+15m^2R^5)]/(15nq\Omega^2) \quad (B.1)$$

$$B(h) = \xi h^3\alpha[80nR^3-7h^3(n+mR^2)+2h^2(21nR+5mR^3)]/(60nq^3\Omega)+16^n\,\mathrm{Re}_n h^6R^3\alpha\Gamma^{-2n} \{-6664n^3mh^5R^8+6080n^4hR^{10}-3840n^4R^{11}-96n^3h^3R^8(97n-19mR^2)+1120n^3h^2R^9 (7n+2mR^2)+14h^{11}(n+mR^2)^2(2n+mR^2)(n+3mR^2)+8nmh^6R^7(183n^2+5m^2R^4) -8n^2h^4R^7(684n^2+677nmR^2+15m^2R^4)+2nmh^5R^4(522n^2+188nmR^2+62m^2R^4) +8n^2h^7R^4(141n^2+158m^2R^4)+2nmh^{10}R^3(526n^2+575nmR^2+222m^2R^4)-2h^8R^3 (-258n^4+n^3mR^2-85n^2m^2R^4+95nm^3R^6+15m^4R^8)+h^5R[287n^4h^5+591n^4h^4R +60n^4hR^4+4n^3R^5(745mh^2+219n)+m^2hR^8(59m^2h^4-988n^2)-m^2R^9(13m^2h^4 +12nmh^2+1716n^2)]\}/(720n^2q^3\Omega^5)+\mathrm{Re}\,\alpha\beta^2h^3R^2[80nR^3-7h^3(n+mR^2)-2h^2R (21n+5mR^2)]/(120nq^2\Omega) \quad (B.2)$$

$$C(h) = \xi\alpha^3h^3[80nR^3-7h^3(n+mR^2)-2h^2R(21n+5mR^2)]/(15nq\Omega) \quad (B.3)$$

$$D(h) = \xi h^2\alpha[80n^2hR^5-240n^2R^6+7h^6(n+mR^2)(2n+mR^2)+10nh^2R^4(13n+mR^2) +8nh^3R^3(10n+9mR^2)+h^5(49n^2R+52nmR^3+19m^2R^5)+h^4(35n^2R^2+66nmR^4 +15m^2R^6)/(30nq^4\Omega^2)+16^n\,\mathrm{Re}_n h^5R^2\alpha\Gamma^{-2n}\{-62080n^5hR^{13}+46080n^5R^{14} +384n^4h^3R^{11}(289n-133mR^2)-70h^{14}(n+mR^2)^2(2n+mR^2)^2(n+3mR^2)-640n^4h^2R^{12} (289n+80mR^2)+32n^3h^4R^{10}(8536n^2+4903nmR^2+215m^2R^4)+8n^3h^5R^8(2551n^2 +28752nmR^2+6157m^2R^4)-120n^2h^6R^8(795n^3+372n^2mR^2-323nm^2R^4+8m^3R^6) -2h^{13}R(n+mR^2)(2n+mR^2)(532n^3+1411nm^2R^2+840nm^2R^4+265m^3R^6)-8n^2h^7R^7 (5790n^3+18627n^2mR^2+5235nm^2R^4+331m^3R^6)-6nh^9R^5(2343n^4+2802n^3mR^2 +2386n^2m^2R^4+1074nm^3R^6-101m^4R^8)-8nh^8R^6(2388n^4+12441n^3mR^2+561nm^3R^6 -95m^4R^8)-2h^{10}R^4(5945n^5+24546n^4mR^2+21834n^3m^2R^4+9006n^2m^3R^6 +609nm^4R^8-60m^5R^{10})-2h^{11}R^3(596n^5+7058n^4mR^2+9726n^3m^2R^4+4839n^2m^3R^6 +990nm^4R^8+118m^5R^{10})-2h^{12}R^2(996n^5+19n^4mR^2+3264n^3m^2R^4+3633n^2m^3R^6 +1428nm^4R^8+122m^5R^{10})-mh^7R^4[10716n^4R^5-4196n^2m^2R^9-12n^2hR^4(6493n^2 -2608nmR^2+865m^2R^4)+h^5(4333n^4+71m^4R^8)-h^4(4853n^4R+361m^4R^9)]\} /(720n^2q^4\Omega^6)+\mathrm{Re}\,\alpha\beta^2h^2R^2\{480n^2R^6-21h^6(n+mR^2)(n+mR^2)-20h^2R^4(21n+mR^2) -6mh^4R^4(21n+5mR^2)-84h^3(R^3+mR^5)-8h^5R[21n^2+mR^2(19n+6mR^2)]\}/(120nq^3\Omega^2) \quad (B.4)$$

$$E(h) = \xi\alpha^3h^2[240n^2R^5-160n^2hR^4-2nh^3R^2(mR^2-63n)-14h^5(n+mR^2)(mR^2+2n) -10nh^2R^3(mR^2+13n)+h^4(91n^2R+58nmR^3+15m^2R^5)]/(15nq\Omega^2) \quad (B.5)$$

廣義型黏滯磁流體薄膜具弱非線性效應於旋轉垂直圓柱穩定性分析

林銘哲
國立高雄科技大學(建工校區)機械系

鄭博仁
遠東科技大學機械系

摘要

本文檢驗廣義型黏滯流體薄膜具弱非線性效應於旋轉垂直圓柱之液磁穩定性，數學建模選用冪次律模型流體做為在外加均勻磁場作用下分析高分子光阻劑流變行為，並利用長波擾動技巧得到該流體系統之無因次廣義自由面運動方程式。Ginzburg-Landau 方程式用來數值解析並圖示各種流動狀態之臨界條件，並探討漢特曼數(Hartmann constant)、羅斯比數(Rossby number)及流動指數(flow index)在小雷諾數流動下對高分子光阻劑磁液動穩定性之影響。再者，當相同塗層流動條件下，增加磁場效應，研究結果指出脹流性流體(dilatant fluid)比擬塑性流體(pseudo plastic fluid)較具穩定作用。